A MIMO-OFDM Digital Baseband Receiver Design with Adaptive Equalization Technique for IEEE 802.16 WMAN

Fang-Li Yuan, Chin-Hsien Lin, Yi-Hsien Lin, Chih-Feng Wu and Chorng-Kuang Wang, *Fellow*, *IEEE*
Graduate Institute of Electronics Engineering and Department of Electrical Engineering,
National Taiwan University, Taipei, Taiwan (flyuan, chlin, ckdarren, cfwu@aic.ee.ntu.edu.tw and ckwang@cc.ee.ntu.edu.tw)

***Abstract*— In this paper, a 2×2 MIMO-OFDM digital baseband receiver for IEEE 802.16 WMAN-OFDM PHY is presented. The inner receiver design includes the timing and carrier frequency synchronization, the channel estimation and the MIMO detection with adaptive equalization technique. In order to enhance the robustness of the system, the BLMS algorithm is derived to track the channel variation for the Alamouti-scheme STBC FEQ. The simulation results demonstrate that the MIMO receiver with adaptive equalization technique has superior SER performance over frequency selective fading channel.**

***Index Terms*—MIMO, OFDM, STBC, BLMS**

I. Introduction

Multiple-input multiple-output (MIMO) technique has been utilized in combination with OFDM technology for wireless communication systems to enhance the link throughput as well as the robustness of transmission over frequency selective fading channel. This technology has been employed in the physical layer (PHY) specification of IEEE 802.16 standard to provide fixed broadband wireless access services. According to the optional specification, Alamouti-scheme space-time block code (STBC) [1] is adopted to realize the 2×1 MISO transmission. In addition, the receiver with two receive antennas can be designed to improve the system performance by exploiting the property of space diversity [2]. Therefore, a 2×2 MIMO-OFDM system for IEEE 802.16 Wireless Metropolitan Area Network (WMAN) is considered in this paper.

Recently, there have been many approaches focusing on the design of MIMO-OFDM systems [3][4]. However, none of them applies the adaptive equalization for enhancing the robustness of the system. Although the initial channel information can be acquired from the channel estimation, there is still a certain estimation error caused by the synchronization error and the additive white Gaussian noise (AWGN). On the other hand, unlike the typical assumption that the channel is quasi-stationary throughout the entire frame, the channel is in reality having a little bit of variation from symbol to symbol even under the environment with slight Doppler effect. Therefore, in order to provide reliable information for the equalization process, a well-designed system has to adaptively track and rectify the estimated channel coefficients.

In this paper, a MIMO-OFDM digital baseband receiver for IEEE 802.16 WMAN is presented. Based on the previous work [5], which focus on the single-input single-output (SISO) system, algorithms for synchronization and channel estimation considering the MIMO case are designed and simulated. The frequency-domain equalizer (FEQ) with adaptive equalization technique is also employed. The paper is organized as follows: the system description is introduced in section II. Next, the receiver architecture is presented in section III. The simulation result is given in section IV. Finally, the conclusion is shown in section V.

TABLE I
System parameter of WMAN-OFDM PHY

Item	Sym.	ETSI	MMDS	WCS
Frequency Band (GHz)		(1)10.00~10.68 (2)3.410~4.200	2.150~2.162 2.500~2.690	2.305~2.320 2.345~2.360
Sampling Factor	n	8/7	86/75	144/125
Transmission Bandwidth (MHz)	BW	(1)3.5, 7, 14, 28 (2)1.75	1.5, 3.0, 6.0, 12.0, 24.0	2.5, 5.0, 10.0, 15.0
Sampling Frequency	F	floor(n×BW/8000)×8000		
Modulation		QPSK, 16-QAM, 64-QAM		
Number of Subcarrier	N	256 (data: 192, pilot: 8, null: 56(−128~−101, 0, 101~127))		
Pilot Tone Index		±13, ±38, ±63, ±88		
Guard Interval Ratio	G	1/4, 1/8, 1/16, 1/32		
Subcarrier Spacing	Δf	F/N		
Useful Symbol Duration	T_b	$1/\Delta f$		
Cyclic Prefix Duration	T_g	$G \times T_b$		
OFDM Symbol Duration	T_s	$T_b + T_g$		

MMDS: Multipoint Microwave Distribution System WCS: Wireless communications service
ETSI: European Telecommunications Standards Institute

II. System Description

A. System Parameters

According to the specification of WMAN-OFDM PHY [6] [7], the total number of subcarriers is 256, including the data, pilot and null parts. Eight BPSK-mapped pilots with indices of $\pm\{13, 38, 63, 88\}$ are used for synchronization purpose. Three constellation mapping types (QPSK and 16/64-QAM) and four guard interval ratios ($\frac{1}{4}$, $\frac{1}{8}$, $\frac{1}{16}$ and $\frac{1}{32}$) are defined to increase the system scalability. Other parameters, including the subcarrier spacing, useful symbol duration, cyclic-prefix (CP) duration and OFDM symbol duration, are determined by the sampling frequency (**F**). Furthermore, the sampling frequency is determined by two parameters: the sampling factor (**n**) and the transmission bandwidth (**BW**). The detailed description of the system parameter is summarized in Table I.

B. Frame Structure and Preamble Format

As shown in Fig. 1, a down-link (DL) PHY protocol data unit (PDU) starts with a long preamble, which is transmitted

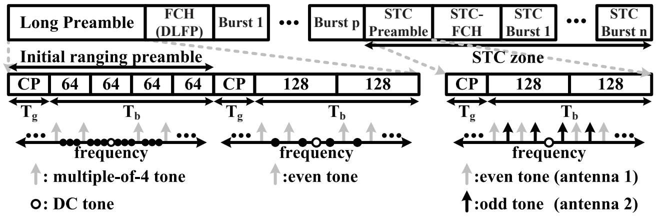

Fig. 1. Frame structure and preamble format

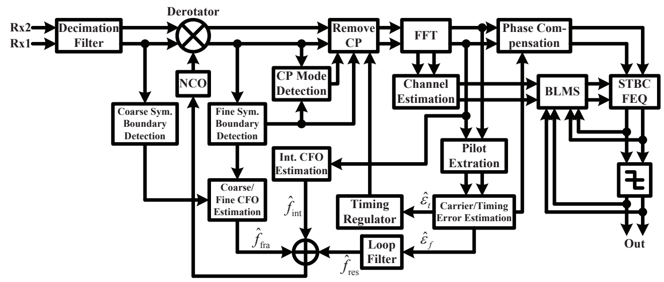

Fig. 2. Receiver architecture for 2×2 MIMO-OFDM

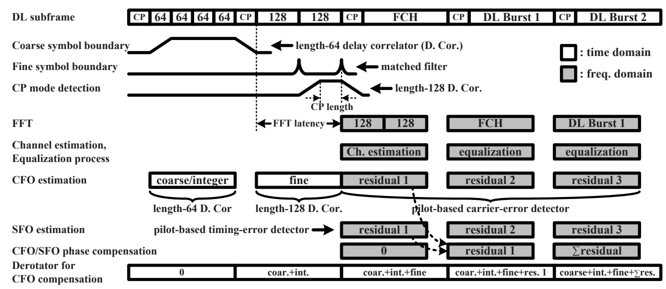

Fig. 3. Scheduling of receiver signal processing

by a single antenna. The preamble is followed by a frame control header (FCH) burst, which contains the DL frame prefix (DLFP) to specify the burst profile and the length of DL bursts immediately following the FCH. DLFP also specifies the start time of the space-time coding (STC) zone, where the DL bursts are transmitted by two antennas based on Alamouti-scheme STBC. The STC zone starts from an STC preamble, which is used for channel estimation in MIMO transmission mode. Finally, the STC bursts are transmitted until the frame ends.

The first part of the long preamble, i.e. the initial ranging preamble, is transmitted by subcarriers whose indices are a multiple of four. As a result, the time-domain waveform of it consists of four repetitions of 64-sample fragment. Similarly, the second part utilizes only even subcarriers, and its time-domain waveform is composed of two 128-sample sequences. Finally, the STC preamble is transmitted from both of the transmit antennas simultaneously, with the reference signals for the 1$^{\text{st}}$ and the 2$^{\text{nd}}$ antenna being transmitted on even and odd tones, respectively.

III. Receiver Architecture

The MIMO receiver architecture is depicted in Fig. 2. Since the frame is configured to start with the SISO transmission, the first receiver path is used for initial synchronization. Note that there is no need to perform coarse and fine synchronization in MIMO transmission mode since the received data have been initially synchronized in SISO case. Namely, only the residual error tracking has to be performed.

The scheduling of the receiver is shown in Fig. 3. There are five important steps for receiver signal processing. First of all, the data are fed into the length-64 delay correlator to detect the coarse symbol boundary. Second, the coarse/integer/fine carrier frequency offset (CFO) detection is performed sequentially. After that, the CFO compensation is done by feeding the frequency offset information into the numerically-controlled oscillator (NCO) and then derotating the received signals. Fourth, the fine symbol boundary and CP mode detection are employed to deliver the correct set of data for demodulation. Finally, after transforming the data into frequency-domain symbols, the channel estimation and adaptive equalization are used for data recovery. Meanwhile, information given by the pilots is fed into the carrier synchronization loop (CSL), the timing regulator and the phase compensation blocks to eliminate the residual CFO and sampling frequency offset (SFO). Synchronization algorithms for the SISO system can be found in [5][8][9]. In the following subsections, the functional blocks focusing on the MIMO signal processing are introduced.

A. Demodulation

The demodulation is performed by the 256-point fast Fourier transform (FFT) operation [11]. As for the practical implementation, an FFT processor capable of dealing with two data sequences is needed. The 2×2 MIMO-FFT processor in the system is implemented by the mixed-radix dataflow scheduling (MRDS) architecture, which can significantly reduce the hardware complexity compared with other works [12].

B. Synchronization for Residual Error Tracking

1) Residual CFO and SFO Estimation: According to [9], the inter-carrier interference (ICI) caused by CFO and SFO is small and can be neglected when only the residual part is left. Therefore, the frequency-domain expression of the residual CFO and SFO can be written as follows (without considering AWGN for simplicity):

$$Y_q^l\left(k\right) = \sum_{p=1}^{2}\left[H_{qp}\left(k\right)X_p^l\left(k\right)\right]\operatorname{sinc}\left(\zeta\right)e^{j\pi\left(\frac{1-N}{N}\right)\zeta}e^{j2\pi\frac{N_s}{N}\zeta l} \tag{1}$$

, where $\zeta = \varepsilon_f + k\varepsilon_t$, ε_f denotes the normalized CFO with respect to the subcarrier spacing, ε_t represents the sampling point offset caused by SFO, p and q are indices of the transmit and the receive antenna, k is the subcarrier index, l and N_s represent the index and the length of the OFDM symbol. The transmitted and received data are represented by $X(\cdot)$ and $Y(\cdot)$, respectively. $H_{qp}(\cdot)$ denotes the channel frequency response from the pth transmit to the qth receive antenna.

Considering the STBC structure of BPSK-mapped pilots, the received signals can be formulated as

$$\begin{aligned} Y_q^{l_{even}}\left(k\right) &= \pm\left[H_{q2}\left(k\right)+H_{q1}\left(k\right)\right]\varphi e^{j2\pi\frac{N_s}{N}\zeta l_{even}} \\ Y_q^{l_{odd}}\left(k\right) &= \pm\left[H_{q2}\left(k\right)-H_{q1}\left(k\right)\right]\varphi e^{j2\pi\frac{N_s}{N}\zeta l_{odd}} \end{aligned} \tag{2}$$

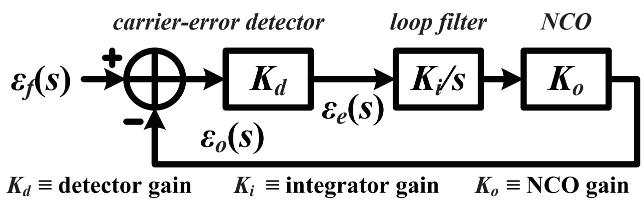

Fig. 4. Equivalent s-domain closed-loop model of the carrier synchronization loop

where $k \in \pm\{13, 38, 63, 88\}$ and $\varphi = \operatorname{sinc}(\zeta)\, e^{j\pi\left(\frac{1-N}{N}\right)}$. Based on this derivation, the carrier/timing-error estimation is employed to estimate the residual CFO and SFO by taking the phase difference between adjacent "even" or "odd" OFDM symbols on each subchannel:

$$\begin{aligned}\Psi_q^{l_{even/odd}}(k) &= \angle\left[Y_q^{l_{even/odd}}(k) \times Y_q^{l_{even/odd}-2}(k)^*\right] \\ &= \tfrac{4\pi N_s}{N}\left(\varepsilon_f + k\varepsilon_t\right).\end{aligned} \quad (3)$$

Obviously, the CFO and SFO can be estimated by taking the mean and the slope of estimation results from pilots, respectively.

2) Carrier Synchronization Loop: The CSL is employed to compensate the residual CFO. It consists of three parts, including the carrier-error detector, loop filter and NCO. Note that the carrier-error detector is composed of functional blocks along the datapath from derotator to carrier-error estimation. The loop filter is realized with an integrator, and the equivalent closed-loop model is depicted in Fig. 4. Obviously, the CSL is a first-order closed-loop with the following transfer function:

$$H(s) = \frac{K_d K_i K_o}{s + K_d K_i K_o}. \quad (4)$$

Considering the discrete-time description of CSL, Eq. (4) can be written as

$$H(z) = H(s)\big|_{s=\frac{1-z^{-1}}{T}} = \frac{K_d K_i K_o T}{K_d K_i K_o T + 1 - z^{-1}} \quad (5)$$

where $T = \frac{1}{F}$ denotes the sampling period.

3) Phase Compensation and Timing Regulation: Because CSL is essentially a frequency-locked loop, the phase compensation block is used to deal with the cumulative frequency error from the residual CFO/SFO with the following expression:

$$\theta_q^l(k) = \sum_{i=0}^{l-1} \Psi_q^i(k) \quad (6)$$

where $\theta_q^l(k)$ denotes the phase correction term on the kth subchannel of the lth OFDM symbol for the qth receiver path. On the other hand, though the rotation effect caused by SFO has been compensated in frequency domain, the SFO still gradually shifts the symbol boundary forward or backward. Therefore, the receiver would receive one more or less sample with respect to the transmitter at a certain moment. Accordingly, the timing regulator is employed to adjust the symbol boundary whenever the summation of the estimated sampling point offset ($\hat{\varepsilon}_t^i$) exceeds one sample duration, i.e.

$$\eta = \min\left\{ l \,|\, l \in \mathrm{N},\, N_s \sum_{i=\eta_0}^{\eta_0+l-1} \left|\hat{\varepsilon}_t^i\right| \geq 1 \right\} \quad (7)$$

where η and η_0 denotes the current and the last period for timing adjustment, respectively.

C. Channel Estimation

Considering the structure of STC preamble, the transmitted training symbols from the two antennas are orthogonal to each other. Therefore, H_{11} (and H_{21}) can be estimated by computing the least-square (LS) estimation and the piecewise-parabolic interpolation on even and odd subchannels, respectively. Similarly, H_{12} (and H_{22}) are estimated by the LS estimation and the interpolation on odd and even tones.

D. BLMS Adaptive Equalization

When the receiver is operated in MIMO transmission mode, the received symbols on each subchannel can be expressed as follows:

$$\begin{aligned}\begin{bmatrix} Y_1^l & Y_1^{l+1} \\ Y_2^l & Y_2^{l+1} \end{bmatrix} &= \begin{bmatrix} H_{11} & H_{12} \\ H_{21} & H_{22} \end{bmatrix} \begin{bmatrix} X_1^l & X_1^{l+1} \\ X_2^l & X_2^{l+1} \end{bmatrix} \\ &= \begin{bmatrix} H_{11} & H_{12} \\ H_{21} & H_{22} \end{bmatrix} \begin{bmatrix} X_1^l & -(X_2^l)^* \\ X_2^l & (X_1^l)^* \end{bmatrix}\end{aligned} \quad (8)$$

where $*$ denotes the complex conjugate. Subsequently, the decoding algorithm can be derived as

$$\begin{bmatrix} \hat{X}_1^l \\ \hat{X}_2^l \end{bmatrix} = \frac{1}{\sigma} \begin{bmatrix} \hat{H}_{11}^* & \hat{H}_{12} & \hat{H}_{21}^* & \hat{H}_{22} \\ \hat{H}_{12}^* & -\hat{H}_{11} & \hat{H}_{22}^* & \hat{H}_{21} \end{bmatrix} \begin{bmatrix} Y_1^l \\ \left(Y_1^{l+1}\right)^* \\ Y_2^l \\ \left(Y_2^{l+1}\right)^* \end{bmatrix} \quad (9)$$

where $\hat{H}_{qp}$ denotes the estimated channel frequency response. σ is the normalization factor, which is equal to the total channel power from all of the paths, i.e. $\sigma = \sum_{q=1}^{2}\sum_{p=1}^{2}\left|\hat{H}_{qp}\right|^2$.

Since the subchannel response is expressed in the matrix form, it is not suitable for tracking and updating the channel variation. Accordingly, Eq. (9) has to be reformulated as follows:

$$\begin{bmatrix} \hat{X}_1^l \\ \left(\hat{X}_2^l\right)^* \end{bmatrix} = \begin{bmatrix} Y_1^l & -Y_1^{l+1} \\ \left(Y_1^{l+1}\right)^* & \left(Y_1^l\right)^* \\ Y_2^l & -Y_2^{l+1} \\ \left(Y_2^{l+1}\right)^* & \left(Y_2^l\right)^* \end{bmatrix}^T \left(\frac{1}{\sigma} \begin{bmatrix} \hat{H}_{11}^* \\ \hat{H}_{12} \\ \hat{H}_{21}^* \\ \hat{H}_{22} \end{bmatrix} \right) \quad (10)$$

$$\hat{\mathbf{X}}_1 = \mathbf{Y}_1 \hat{\mathbf{H}}_1$$

Clearly, the decoding symbol vector ($\hat{\mathbf{X}}_1$) in Eq. (10) is equal to a 2×4 received symbol matrix ($\mathbf{Y}_1$) multiplied by the channel response vector ($\hat{\mathbf{H}}_1$). Note that the initial condition of $\hat{\mathbf{H}}_1$ is equal to the estimated subchannel response vector divided by the normalization factor σ. Finally, BLMS algorithm [13][14] is described as

$$\tilde{\mathbf{X}}_1 = Q\left[\hat{\mathbf{X}}_1\right],\ Q[\bullet] \equiv \text{slicer} \quad (11)$$

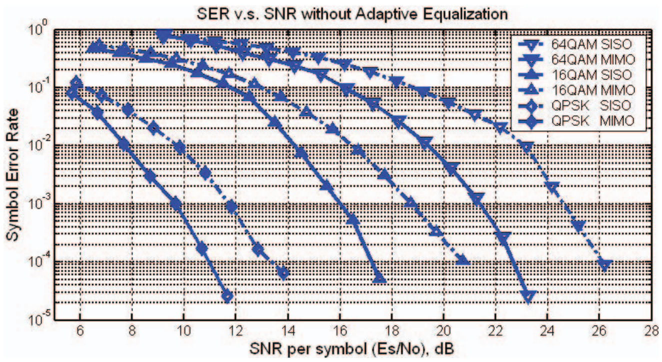

Fig. 5. SER comparisons between SISO and MIMO transmissions (SUI3 channel, ± 16 ppm CFO/SFO, 32 MHz sampling frequency without adaptive equalization)

$$\hat{\mathbf{H}}_{\mathbf{l+2}} = \hat{\mathbf{H}}_{\mathbf{l}} + \mu \mathbf{Y}_{\mathbf{l}}^{\mathbf{H}} \left(\tilde{\mathbf{X}}_{\mathbf{l}} - \hat{\mathbf{X}}_{\mathbf{l}} \right) \tag{12}$$

where the step-size parameter μ is used for managing the tradeoff between the convergence property and the value of misadjustment. Note that $\hat{\mathbf{H}}_{\mathbf{l}}$ is updated at every block of two OFDM symbols, and this is why BLMS gets its name.

IV. Simulation Result

The design has been simulated based on the system parameters of IEEE 802.16 WMAN. The sampling and the carrier frequency are 32 MHz and 10.68 GHz respectively, based on European Telecommunications Standards Institute (ETSI). Subsequently, the strength of CFO and SFO is 16 ppm of the carrier and sampling frequency, which is the maximal tolerable value defined by the IEEE 802.16 standard. In addition, the Stanford University Interim (SUI) channel model is employed to build up the simulation environment of the wireless multipath fading channel.

The comparisons of SER performance between SISO and MIMO transmissions are shown in Fig. 5. It is clear that the MIMO transmission has superior performance improvement by about 3 dB compared with the SISO case at 10^{-4} SER. On the other hand, the comparisons of MIMO transmission between using BLMS adaptive equalization or not are given in Fig. 6. According to the simulation results, the STBC-based BLMS adaptive FEQ improves the SER performance (about 2 dB at 10^{-4} SER) as well as the system robustness over non-adaptive ones.

V. Conclusion

A 2×2 MIMO-OFDM digital baseband receiver design for IEEE 802.16 WMAN-OFDM PHY is presented. The inner receiver design includes the coarse/fine synchronization, residual CFO/SFO estimation/compensation, MIMO channel estimation, Alamouti-scheme STBC detector and BLMS adaptive equalization. Based on the format of STC preamble, the frequency response of the 2×2 MIMO channel can be easily estimated by performing LS estimation and the piecewise-parabolic interpolation. On the other hand, BLMS algorithm is derived to adaptively track the channel variation for the STBC-based FEQ. The simulation results show the performance enhancement of the MIMO receiver over frequency selective fading channel.

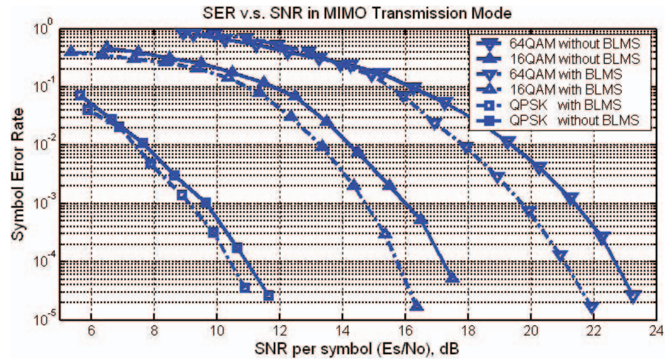

Fig. 6. SER comparisons of BLMS adaptive equalization (2×2 MIMO transmission, SUI3 channel, ± 16 ppm CFO/SFO, 32 MHz sampling frequency)

Acknowledgment

This work was supported in part by the National Science Council, Taiwan, under Grand NSC 96-2220-E-002-001.

References

[1] S. M. Alamouti, "A Simple Transmit Diversity Technique for Wireless Communications," *IEEE J. Selected Areas in Comm.*, vol. 16, no. 8, pp. 1451-1458, Oct. 1998.
[2] A. Paulraj, R. Nabar and D. Gore, "Introduction to Space-Time Wireless Communications," cambridge 2003.
[3] Zih-Yin Ding, Chi-Yun Chen and Tzi-Dar Chiueh, "Design of a MIMO-OFDM Baseband Receiver for Next-Generation Wireless LAN," *in proc. IEEE Int. Symposium on Circuits and Systems (ISCAS)*, May 2006.
[4] Jui-Ping Lien, Po-An Chen and Tzi-Dar Chiueh, "Design of a MIMO OFDM Baseband Transceiver for Cognitive Radio System," *in proc. IEEE Int. Symposium on Circuits and Systems (ISCAS),* May 2006.
[5] M. Speth, S. A. Fechtel, G. Fock and H. Meyr, "Optimum Receiver Design for Wireless Broad-Band Systems Using OFDM – Part I," *IEEE Trans. on Comm.*, vol. 47, no. 11, pp. 1668-1677, Nov. 1999.
[6] IEEE 802.16-2004, "IEEE Standard for Local and Metropolitan Area Networks - Part 16: Air Interface for Fixed Broadband Wireless Access Systems", Oct. 2004.
[7] IEEE 802.16e-2005, "IEEE Standard for Local and metropolitan area networks Part 16: Air Interface for Fixed and Mobile Broadband Wireless Access Systems Amendment 2: Physical and Medium Access Control Layers for Combined Fixed and Mobile Operation in Licensed Bands and Corrigendum 1", Feb. 2006.
[8] T. M. Schmidl and D. C. Cox, "Robust Frequency and Timing Synchronization for OFDM," *IEEE Trans. on Comm.*, vol. 45, no. 12, pp. 1613-1621, Dec. 1997.
[9] M. Speth, S. A. Fechtel, G. Fock and H. Meyr, "Optimum Receiver Design for Wireless Broad-Band Systems Using OFDM – Part II: A Case Study," *IEEE Trans. on Comm.*, vol. 49, no. 4, pp. 571-578, Apr. 2001.
[10] P. Y. Tsai and T. D. Chiueh, "Frequency Domain Interpolation-Based Channel Estimation in Pilot-Aided OFDM Systems," *in proc. IEEE Vechicular Technology Conference*, vol. 1, pp. 420-424, May 2004.
[11] J. W. Cooley and J. W. Tukey, "An Algorithm for the Machine Calculation of Complex Fourier Series, " *Math. Comp.*, vol. 19, pp. 297-301, 1965.
[12] Fang-Li Yuan, Yi-Hsien Lin, Chih-Feng Wu, Muh-Tian Shiue and Chorng-Kuang Wang, "A 256-Point Dataflow Scheduling 2×2 MIMO FFT/IFFT Processor for IEEE 802.16 WMAN," *in proc. IEEE Asian Solid-State Circuits Conference (A-SSCC),* pp. 309-312, Nov. 2008.
[13] W. M. Younis, N. Al-Dhahir and A. H. Sayed, "Adaptive Frequency-Domain Equalization of Space-Time Block-Coded Transmissions," *in proc. IEEE Int. Conf. Acoustics, Speech and Signal Processing (ICASSP)*, vol. 3, pp. 2353-2356, May 2002.
[14] S. Haykin, "Adaptive Filter Theory," 4th Edition, Prentice-Hall, 2002.